Article

Abraham Solvation Parameter Model: Calculation of L Solute Descriptors for Large C_{11} to C_{42} Methylated Alkanes from Measured Gas–Liquid Chromatographic Retention Data

Emily Wu, Sneha Sinha, Chelsea Yang, Miles Zhang and William E. Acree, Jr. *

Department of Chemistry, University of North Texas, Denton, TX 76203, USA; emilywu@my.unt.edu (E.W.);
snehasinha@my.unt.edu (S.S.); chelseayang@my.unt.edu (C.Y.); mileszhang@my.unt.edu (M.Z.)
* Correspondence: bill.acree@unt.edu

Abstract: Abraham model **L** solute descriptors have been determined for 149 additional C_{11} to C_{42} monomethylated and polymethylated alkanes based on published Kovat's retention indices based upon gas–liquid chromatographic measurements. The calculated solute descriptors, in combination with previously published Abraham model correlations, can be used to predict a number of very important chemical and thermodynamic properties including partition coefficients, molar solubility ratios, gas–liquid chromatographic and HPLC retention data, infinite dilution activity coefficients, molar enthalpies of solvation, standard molar vaporization and sublimation at 298 K, vapor pressures, and limiting diffusion coefficients. The predictive computations are illustrated by estimating both the standard molar enthalpies of sublimation and the enthalpies of solvation in benzene for the monomethylated and polymethylated alkanes considered in the current study.

Keywords: Abraham model; solute descriptors; polymethylated alkanes; enthalpies of vaporization; enthalpies of solvation; enthalpies of sublimation

1. Introduction

Scientists and engineers in both academia and the industrial manufacturing sector must rely upon empirical and semi-theoretical models to predict the thermodynamic and physical properties required in process design calculations. Even with today's modern instrumentation it is not feasible to experimentally determine the properties for the more than 60 million known chemical compounds [1]. Chemical manufacturing processes rarely contain only a single compound. Experimental measurements become even more challenging when one takes into account the number of possible binary, ternary and higher-order multicomponent mixtures that can be prepared from existing compounds. The number of possible combinations increases annually as new compounds are synthesized, found and identified.

Over the last 50 years numerous predictive methods have been developed based upon either quantitative structure–property relationships (QSPRs) or group contribution concepts. QSPR methods [2–8] identify mathematical relationships between the desired property that one wishes to calculate and other physical properties or from compound descriptor values that can be derived from molecular structure and/or quantum mechanical considerations. For some published QSPR studies [2,6,8] more than 1000 different descriptors have been considered before narrowing the descriptor set down to those yielding the desired predictive accuracy. Group contribution methods [9–16], on the other hand, fragment the given molecule into atoms or functional groups. A numerical value is then assigned to each atom or fragment group. In the simplest case the desired property would be calculated as the summation of the product of the number of occurrences each fragment group appears in the molecule times its respective numerical group value. Naturally the method would be limited to those molecules having known functional group values.

The predictive method that we have been using to predict thermodynamic and physical properties is based upon the Abraham solvation parameter model [17–20] which defines solute transfer between two immiscible (or partly miscible) phases in terms of a linear free energy relationship (LFER). The first LFER:

$$\text{Solute Property} = e_1 \times \mathbf{E} + s_1 \times \mathbf{S} + a_1 \times \mathbf{A} + b_1 \times \mathbf{B} + v_1 \times \mathbf{V} + c_1 \qquad (1)$$

describes solute transfer between two condensed phases, while the second LFER:

$$\text{Solute Property} = e_2 \times \mathbf{E} + s_2 \times \mathbf{S} + a_2 \times \mathbf{A} + b_2 \times \mathbf{B} + l_2 \times \mathbf{L} + c_2 \qquad (2)$$

describes solute transfer into a condensed phase from the gas phase. Specific properties that have been successfully described include partition coefficients [20–22], molar solubility ratios [19,23,24], aquatic toxicities [25–27], nasal pungencies [28], gas–liquid chromatographic and HPLC retention data [18,29–33], Draize scores and eye irritation thresholds [34,35], human and rat intestinal adsorption data [36,37], human skin permeability [38,39], infinite dilution activity coefficients [40,41], molar enthalpies of solvation [42–44], standard molar vaporization [45] and sublimation [46] at 298 K, vapor pressures [47], and limiting diffusion coefficients [48,49].

Unlike many of the QSPRs that have been proposed in the published chemical and engineering literature, Equations (1) and (2) are based upon a fundamental understanding of how molecules interact in solution. The first five terms on the right-hand side of both Equations (1) and (2) represent a different type of molecular interaction that is described by the product of a solute property ($\mathbf{E}$, $\mathbf{S}$, $\mathbf{A}$, $\mathbf{B}$, $\mathbf{V}$ and $\mathbf{L}$) times its complimentary solvent or process property (e_1, s_1, a_1, b_1, v_1, c_1, e_2, s_2, a_2, b_2, l_2 and c_2). The uppercase alphabetical characters in both Abraham model correlations are called solute descriptors, and are defined in the following manner: $\mathbf{A}$ and $\mathbf{B}$ represent the respective overall hydrogen-bond donating and accepting abilities of the dissolved solute; $\mathbf{E}$ denotes the given solute's excess molar refraction referenced to that of a linear alkane having a comparable molecular size; $\mathbf{L}$ refers to the logarithm of the solute's gas-to-hexadecane partition coefficient determined at 298.15 K; $\mathbf{S}$ corresponds to a combination of the electrostatic polarity and polarizability of the solute; and $\mathbf{V}$ is the solute's McGowan molecular volume calculated from known sizes of the constituent atoms and chemical bond numbers. The numerical values of the lowercase solvent or process property are determined by a least-squares analysis that involves curve-fitting the measured property for a series of solutes with known descriptor values in a given solvent (or for a given process) in accordance with Equations (1) and (2) of the Abraham model. The calculated numerical values of solvent/process equation coefficients depend upon the organic solvent or process under consideration. In other words, the equation coefficients that describe the enthalpy of solvation of organic solutes dissolved in benzene are numerically different than the values that describe the enthalpy of solvation of organic solutes in dimethyl sulfoxide. The Abraham model is described in greater detail elsewhere [17,18,50–52].

One major advantage that the Abraham model offers over most predictive QSPRs is that the same numerical values of the solute descriptors are used in every Abraham model correlation, irrespective of the chemical property being predicted. This feature avoids having to calculate a new set of solute descriptors every time that one wishes to predict a different chemical property. A common set of solute descriptors for every correlation also permits one to directly compare the solubilizing properties of different organic solvents and two-phase partitioning systems through Principal Component Analysis, the Euclidean distance formula and other computational methods. Such comparisons might be used to assist design engineers in identifying less toxic, more environmentally compatible solvent alternatives to replace the more hazardous organic solvents currently used in industrial manufacturing processes, or to help in identifying partition systems that might mimic biological response properties. These latter comparisons have involved skin permeation and water-to-organic solvent systems [38], parallel artificial membrane permeability assays and

biological systems [53], and aquatic toxicity and water-to-organic solvent systems [25,27]. Each of the fore-mentioned comparisons described both the specified biological and chemical process in terms of an Abraham model correlation.

At present, experimental-based solute descriptors are available for more than 8500 different molecular organic and organometallic compounds and for more than 300 different ionic species (such as tetraalkylammonium and substituted-pyridinium cations, substituted-phenolate and substituted-benzoate anions), which is only a tiny fraction of the known chemical compounds. Recognizing that it will never be possible to perform a sufficient number of experimental measurements to calculate experimental-based Abraham model solute descriptors for every known chemical compound, researchers have searched for alternative methods to estimate the numerical values. Published group contribution [53–56] and machine learning methods [55,56] have exhibited remarkable promise in that both the molar enthalpies of solvation (ΔH_{solv}) and molar Gibbs energies of solvation (ΔG_{solv}) of molecular organic solutes and inorganic gases in a wide range of organic solvents of varying polarity and hydrogen-bonding character could be reasonably predicted by the estimated solute descriptors. In the study by Chung and coworkers [56] the authors used an "inhouse" solute descriptor database containing 8366 unique chemical compounds. The compounds were fragmented into atom-centered (AC) functional groups. Each solute descriptor was then calculated by:

$$\textbf{E, S, A, B or L} = \sum_{i=1}^{N_{atom}} AC_i + \sum_{j=1} RSC_j + \sum_{k=1} LDI_k \tag{3}$$

summing the contributions from all AC groups, with special ring strain corrections (RSC) and long-distance interaction (LDI) groups being added to account for any more advanced structural features that were not fully captured by the atom-centered approach. Halogenated molecules required a slightly different estimation scheme in that the halogenated atoms were replaced by hydrogen atoms prior to the fragmentation. The correction(s) for the halogen atom(s) were added at the end to the calculated solute descriptor of the "non-halogenated compound":

$$\textbf{E, S, A, B or L} = \sum_{i=1}^{N_{atom*}} AC_i + \sum_{j=1} RSC_j + \sum_{k=1} LDI_k + \sum_{l=1}^{N_{halogen}} Halogen_l \tag{4}$$

where $N_{\text{atom*}}$ and N_{halogen} denote the number of non-halogen heavy atoms and the number of halogen atoms in the given molecule, respectively. The numerical values of the individual AC groups, as well as all RSC, LDI and Halogen values, were determined by regressing the known descriptor values in accordance with Equations (3) and (4). The authors developed a machine learning method for estimating solute descriptors. Both predictive methods are very easy to use as the authors provided a link to the computational software. Users simply enter the canonical SMILES code of the molecule into the software. The results of the authors' calculations showed that solute descriptors estimated by the machine learning method provided the better test set predictive values for both ΔH_{solv} and ΔG_{solv} with mean absolute errors of MAE = 3.89 kJ/mole and MAE = 4.184 kJ/mole, respectively. Slightly larger test set errors of MAE = 4.73 kJ/mole (ΔH_{solv}) and MAE = 4.94 kJ/mole (ΔG_{solv}) were noted in the case of the solute descriptors estimated by the authors' group contribution method. The study by Ulrich and Ebert [57] used the slightly smaller Abraham Absolv solute parameter database found on the UFZ-LSER internet website [58] in developing their group contribution and deep machine learning methods for estimating solute descriptors. Methods aimed at predicting the Abraham model process coefficients have had mixed success; in part, because experimental-based correlations have been developed for relatively few organic solvents and biphasic partition systems [59–62].

The continued development of predictive group contribution and machine learning methods for the Abraham model requires the determination of both experimental-based

solute descriptors and experimental-based solvent/process correlations. Additional experimental measurements are also needed for testing the limitations and applications of new predictive methods. To aid in future endeavors, we have recently reported solute descriptors for an additional 174 monomethyl branched alkanes [63], for an additional 127 C_9–C_{26} mono-alkyl alkanes and polymethyl alkanes [64], for an additional 33 linear C_7–C_{14} alkynes [65], and for several important active pharmaceutical ingredients and intermediates [23,66–68]. Abraham model correlations have also been recently determined for two practical partitioning systems, water-methyl ethyl ketone (MEK) [21] and water-methyl isobutyl ketone (MIBK) [22], and for solute transfer into isopropyl acetate [69], anisole [70] and cyclohexanol [71]. In the current communication we have calculated Abraham model **L** solute descriptor values for an additional 149 C_{11} to C_{44} methylated alkanes from measured gas–liquid chromatographic retention data gathered from a compilation by Katritzky and coworkers [72].

2. Calculation of Abraham Model Solute Descriptors for Methylated Alkanes

Normally the determination of Abraham model solute descriptors involves constructing a series of mathematical expressions for the measured solute properties of the given solute in a series of solvents and/or for a series of processes for which the lowercase equation coefficients are known. The solute properties used in past descriptor calculations have included logarithms of the measured solubility ratio of the solute in several different organic mono-solvents, the logarithms of the measured water-to-organic solvent partition coefficients, measured gas–liquid chromatographic retention data, and/or experimental enthalpies of solvation for the solute dissolved in several different organic solvents. Each of these solute properties will hopefully have very little experimental error. Aquatic toxicities and biological response factors generally have too much experimental error to be used effectively in solute descriptor calculations.

The Abraham model expressions for each of the fore-mentioned processes contain a common set of solute descriptors. The series of mathematical expressions are then solved for the "best" set of descriptor values that minimizes the overall squared-summed difference between the measured properties and the respective back-calculated values based on Equations (1) and (2). For the methylated hydrocarbons listed in Table 1, the computational process is greatly simplified in that the **E**, **S**, **A** and **B** solute descriptors are all equal to zero. The **V** solute descriptor is readily calculated from the solute's molecular structure, the atomic volumes of the constituent atoms contained in the solute molecule, and the number of chemical bonds in the solute molecule as described by Abraham and McGowan [73]. This leaves only the **L** solute descriptor to be calculated.

To calculate the **L** solute descriptor based on the gas–liquid chromatographic data retrieved from the published paper by Katritzky and coworkers [72], we first must establish a mathematical relationship correlation between the reported Kovat's retention indices, KRI, and the **L** solute descriptor for alkane solute molecules. Numerical values KRI are available for 178 methylated alkanes [73]; however, for most of the molecules the **L** solute descriptor is not known. We can increase the number of compounds used in establishing the Abraham model correlation by noting that by definition the KRI values of linear alkanes is simply 100 times the number of carbon atoms. This allows us to add an additional 34 alkanes (heptane through tetracontane) to the regression data set. By combining the 34 linear alkanes and the 29 monomethyl alkanes with known **L** descriptor values from the Katritzky et al. compilation [72], we have 63 experimental data points to use in developing our Abraham model KRI versus **L** descriptor correlation.

Table 1. Kovat's retention indices, KRI, and Abraham model **L** solute descriptors for linear alkanes and for methylated alkanes.

Compound Name	KRI/100	L Value Database	L Value Calculated
Linear Alkanes			
Heptane	7.000	3.173	3.172
Octane	8.000	3.677	3.676
Nonane	9.000	4.182	4.180
Decane	10.000	4.686	4.684
Undecane	11.000	5.191	5.188
Dodecane	12.000	5.696	5.692
Tridecane	13.000	6.200	6.196
Tetradecane	14.000	6.705	6.700
Pentadecane	15.000	7.209	7.204
Hexadecane	16.000	7.714	7.708
Heptadecane	17.000	8.218	8.212
Octadecane	18.000	8.722	8.716
Nonadecane	19.000	9.226	9.220
Eicosane	20.000	9.731	9.724
Heneicosane	21.000	10.236	10.228
Docosane	22.000	10.740	10.732
Tricosane	23.000	11.252	11.236
Tetracosane	24.000	11.758	11.740
Pentacosane	25.000	12.264	12.244
Hexacosane	26.000	12.770	12.748
Heptacosane	27.000	13.276	13.252
Octacosane	28.000	13.780	13.756
Nonacosane	29.000	14.291	14.260
Triacontane	30.000	14.794	14.764
Hentriacontane	31.000	15.321	15.268
Dotriacontane	32.000	15.787	15.772
Tritriacontane	33.000	16.303	16.276
Tetratriacontane	34.000	16.818	16.780
Pentatriacontane	35.000	17.223	17.284
Hexatriacontane	36.000	17.736	17.788
Heptatriacontane	37.000	18.211	18.292
Octatriacontane	38.000	18.686	18.796
Nonatriacontane	39.000	19.270	19.300
Tetracontane	40.000	19.853	19.804
Monomethylalkanes			
2-Methylnonane	9.665	4.453	4.515
3-Methylnonane	9.730	4.486	4.548
2-Methylundecane	11.665	5.516	5.523
3-Methylundecane	11.725	5.550	5.553
2-Methyltridecane	13.665	6.528	6.531
3-Methyltridecane	13.730	6.563	6.564
2-Methylpentadecane	15.665	7.539	7.539
3-Methylpentadecane	15.737	7.577	7.575
2-Methylheptadecane	17.658	8.551	8.544
3-Methylheptadecane	17.740	8.591	8.585
2-Methylnonadecane	19.660	9.563	9.553
3-Methylnonadecane	19.743	9.607	9.594
10-Methylnonadecane	19.430	9.449	9.437
2-Methylheneicosane	21.660	10.571	10.561
3-Methylheneicosane	21.745	10.621	10.603
11-Methylheneicosane	21.410	10.449	10.435
2-Methyltricosane	23.640	11.586	11.559
3-Methyltricosane	23.745	11.635	11.611
8-Methyltricosane	23.670	11.468	11.574
12-Methyltricosane	23.370	11.449	11.422

Table 1. *Cont.*

Compound Name	KRI/100	L Value Database	L Value Calculated
2-Methylpentacosane	25.630	12.599	12.562
3-Methylpentacosane	25.744	12.651	12.619
13-Methylpentacosane	25.345	12.454	12.418
2-Methylheptacosane	27.630	13.611	13.570
3-Methylheptacosane	27.744	13.666	13.627
14-Methylheptacosane	27.330	13.458	13.418
2-Methylnonacosane	29.622	14.626	14.573
3-Methylnonacosane	29.740	14.680	14.633
15-Methylnonacosane	29.315	14.464	14.419
2-Methylhentriacontane	31.615		15.578
3-Methylhentriacontane	31.741		15.641
4-Methylhentriacontane	31.575		15.558
5-Methylhentriacontane	31.500		15.520
6-Methylhentriacontane	31.432		15.486
7-Methylhentriacontane	31.400		15.470
13-Methylhentriacontane	31.308		15.423
16-Methylhentriacontane	31.298		15.418
2-Methyltritriacontane	33.620		16.588
3-Methyltritriacontane	33.745		16.651
4-Methyltritriacontane	33.575		16.566
5-Methyltritriacontane	33.500		16.528
6-Methyltritriacontane	33.437		16.496
13-Methyltritriacontane	33.285		16.420
17-Methyltritriacontane	33.285		16.420
2-Methylpentatriacontane	35.620		17.596
3-Methylpentatriacontane	35.743		17.658
18-Methylpentatriacontane	35.273		17.422
Dimethylalkanes			
3,9-Dimethyltricosane	24.100		11.790
5,9-Dimethyltetracosane	24.850		12.168
3,11-Dimethylpentacosane	26.090		12.793
3,15-Dimethylpentacosane	26.050		12.773
5,11-Dimethylpentacosane	25.820		12.657
5,17-Dimethylpentacosane	25.850		12.672
7,11-Dimethylpentacosane	25.770		12.632
2,6-Dimethylhexacosane	27.040		13.272
4,8-Dimethylhexacosane	26.950		13.227
5,11-Dimethylhexacosane	26.820		13.161
6,10-Dimethylhexacosane	26.780		13.141
7,11-Dimethylhexacosane	26.750		13.126
3,7-Dimethylheptacosane	28.090		13.801
3,15-Dimethylheptacosane	28.050		13.781
5,11-Dimethylheptacosane	27.820		13.665
5,17-Dimethylheptacosane	27.860		13.685
7,13-Dimethylheptacosane	27.740		13.625
9,19-Dimethylheptacosane	27.650		13.580
2,6-Dimethyloctacosane	29.050		14.285
2,10-Dimethyloctacosane	28.990		14.255
4,10-Dimethyloctacosane	28.950		14.235
5,15-Dimethyloctacosane	28.820		14.169
7,13-Dimethyloctacosane	28.730		14.124
3,7-Dimethylnonacosane	30.080		14.804
3,13-Dimethylnonacosane	30.040		14.784
5,13-Dimethylnonacosane	29.820		14.673
5,19-Dimethylnonacosane	29.830		14.678
7,17-Dimethylnonacosane	29.730		14.628
2,6-Dimethyltriacontane	31.050		15.293
2,10-Dimethyltriacontane	30.990		15.263
2,12-Dimethyltriacontane	30.950		15.243
3,7-Dimethyltriacontane	31.080		15.308

Table 1. *Cont.*

Compound Name	KRI/100	L Value Database	L Value Calculated
4,10-Dimethyltriacontane	30.940		15.238
6,10-Dimethyltriacontane	30.750		15.142
3,7-Dimethylhentriacontane	32.090		15.817
3,13-Dimethylhentriacontane	32.030		15.787
3,15-Dimethylhentriacontane	32.090		15.817
5,13-Dimethylhentriacontane	31.805		15.674
5,17-Dimethylhentriacontane	31.820		15.681
7,11-Dimethylhentriacontane	31.702		15.622
11,21-Dimethylhentriacontane	31.629		15.585
2,8-Dimethyldotriacontane	32.970		16.261
4,8-Dimethyldotriacontane	32.920		16.236
6,10-Dimethyldotriacontane	32.730		16.140
8,12-Dimethyldotriacontane	32.660		16.105
9,21-Dimethyldotriacontane	32.620		16.084
14,18-Dimethyldotriacontane	32.575		16.062
3,9-Dimethyltritriacontane	34.030		16.795
3,15-Dimethyltritriacontane	34.090		16.825
5,16-Dimethyltritriacontane	33.800		16.679
5,19-Dimethyltritriacontane	33.820		16.689
7,17-Dimethyltritriacontane	33.700		16.629
11,23-Dimethyltritriacontane	33.624		16.590
2,10-Dimethyltetratriacontane	34.940		17.254
4,16-Dimethyltetratriacontane	34.890		17.229
6,10-Dimethyltetratriacontane	34.738		17.152
8,12-Dimethyltetratriacontane	34.650		17.108
12,22-Dimethyltetratriacontane	34.614		17.089
13,17-Dimethyltetratriacontane	34.550		17.057
3,7-Dimethylpentatriacontane	36.095		17.836
3,15-Dimethylpentatriacontane	36.010		17.793
5,9-Dimethylpentatriacontane	35.800		17.687
5,19-Dimethylpentatriacontane	35.805		17.690
7,17-Dimethylpentatriacontane	35.697		17.635
9,21-Dimethylpentatriacontane	35.610		17.591
2,12-Dimethylhexatriacontane	36.950		18.267
5,17-Dimethylhexatriacontane	36.800		18.191
13,23-Dimethylhexatriacontane	36.610		18.095
3,15-Dimethylheptatriacontane	38.010		18.801
5,19-Dimethylheptatriacontane	37.790		18.690
5,17-Dimethylheptatriacontane	37.800		18.695
13,23-Dimethylheptatriacontane	37.590		18.589
5,17-Dimethyloctatriacontane	38.780		19.189
Trimethylalkanes			
4,8,12-Trimethyltetracosane	25.200		12.345
5,9,13-Trimethylpentacosane	26.100		12.798
4,8,12-Trimethylhexacosane	27.190		13.348
3,7,11-Trimethylheptacosane	28.380		13.948
4,8,12-Trimethyloctacosane	29.180		14.351
3,7,11-Trimethylnonacosane	30.370		14.950
5,13,17-Trimethylnonacosane	30.070		14.799
6,14,18-Trimethyltriacontane	31.000		15.268
3,7,11-Trimethylhentriacontane	32.365		15.956
5,13,17-Trimethylhentriacontane	32.054		15.799
7,13,17-Trimethylhentriacontane	31.913		15.728
11,15,19-Trimethylhentriacontane	31.810		15.676
2,10,16-Trimethyldotriacontane	33.240		16.397
4,12,16-Trimethyldotriacontane	33.160		16.357
6,14,18-Trimethyldotriacontane	32.990		16.271
12,16,20-Trimethyldotriacontane	32.810		16.180
3,7,15-Trimethyltritriacontane	34.365		16.964
5,13,17-Trimethyltritriacontane	34.050		16.805

Table 1. *Cont.*

Compound Name	KRI/100	L Value Database	L Value Calculated
7,11,15-Trimethyltritriacontane	33.890		16.725
11,15,19-Trimethyltritriacontane	33.796		16.677
2,10,16-Trimethyltetratriacontane	35.240		17.405
4,8,12-Trimethyltetratriacontane	35.155		17.362
6,14,18-Trimethyltetratriacontane	34.970		17.269
8,12,16-Trimethyltetratriacontane	34.864		17.215
12,16,20-Trimethyltetratriacontane	34.780		17.173
3,7,15-Trimethylpentatriacontane	36.363		17.971
5,9,13-Trimethylpentatriacontane	36.050		17.813
7,11,15-Trimethylpentatriacontane	35.883		17.729
13,17,21-Trimethylpentatriacontane	35.770		17.672
13,17,23-Trimethylpentatriacontane	35.830		17.702
4,8,16-Trimethylhexatriacontane	37.150		18.368
8,12,16-Trimethylhexatriacontane	36.850		18.216
14,18,22-Trimethylhexatriacontane	36.760		18.171
3,7,15-Trimethylheptatriacontane	38.350		18.972
5,13,17-Trimethylheptatriacontane	38.030		18.811
7,13,19-Trimethylheptatriacontane	37.840		18.715
15,19,23-Trimethylheptatriacontane	37.750		18.670
15,19,23-Trimethyloctatriacontane	38.735		19.166
5,13,17-Trimethylnonatriacontane	40.010		19.809
15,19,23-Trimethylnonatriacontane	39.724		19.665
14,18,22-Trimethyltetracontane	40.710		20.162
Tetramethylalkanes			
3,7,11,15-Tetramethylnonacosane	30.620		15.076
3,7,11,15-Tetramethylhentriacontane	32.610		16.079
4,8,12,16-Tetramethylhentriacontane	32.490		16.019
3,7,11,15-Tetramethyltritriacontane	34.590		17.077
4,8,12,16-Tetramethyltritriacontane	34.480		17.022
3,7,11,15-Tetramethylpentatriacontane	36.580		18.080
7,11,15,19-Tetramethylpentatriacontane	36.280		17.929
9,13,17,21-Tetramethylpentatriacontane	36.170		17.874
11,15,19,24-Tetramethylpentatriacontane	36.050		17.813
6,10,12,16-Tetramethylhexatriacontane	37.230		18.408
8,12,16,20-Tetramethylhexatriacontane	37.130		18.358
10,14,18,22-Tetramethylhexatriacontane	37.035		18.310
3,7,11,15-Tetramethylheptatriacontane	38.550		19.073
7,11,15,19-Tetramethylheptatriacontane	38.230		18.912
9,13,17,21-Tetramethylheptatriacontane	38.130		18.862
11,15,19,24-Tetramethylheptatriacontane	38.030		18.811
10,14,18,22-Tetramethyloctatriacontane	39.000		19.300

Analysis of the values in the second and third columns of Table 1 yielded the following Abraham model expression:

$$\mathbf{L} = 0.504 \ (0.001) \times (KRI/100) - 0.356 \ (0.012)$$
$$(N = 63, \ SD = 0.034, \ R^2 = 1.000 \ \text{and} \ F = 942{,}023) \tag{5}$$

where N is the number of experimental data points used in the linear least-squares analysis, SD is the standard deviation, R^2 is the squared correlation coefficient, and F is the Fisher F-statistic. Standard errors in the slope and intercept are given in parentheses immediately following the respective equation coefficient. Equation (5) back-calculates the **L** values used in the least-squares analysis to within an average absolute deviation of $AAE = 0.025$ and an average error of $AE = -0.006$. Figure 1 depicts the linear plot of the **L** descriptor values versus $KRI/100$ values for the 63 data points used in deriving Equation (5). The derived mathematical relationship then allows the calculation of the **L** solute descriptors of the remaining 149 methylated alkanes. These calculations are summarized in the last

column of Table 1. As an informational note, Katritzky et al. identified the different alkanes by a numerical labelling scheme where the first two digits in the number indicated the length of the longest carbon chain, and each of the next two-digit pairs showed the location of the methyl substituent on the carbon-atom backbone. We named the compounds labelled 22_0822 and 38_162024 as 8-methyltricosane and 15,19,23-trimethyloctatriacontane, respectively. For the first alkane, the placement of a methyl substituent on the 22nd carbon atom would increase the carbon backbone by one carbon atom. For the second alkane, we renumbered the carbon atoms starting at the other end of the carbon backbone to obtain a smaller set of numerical values.
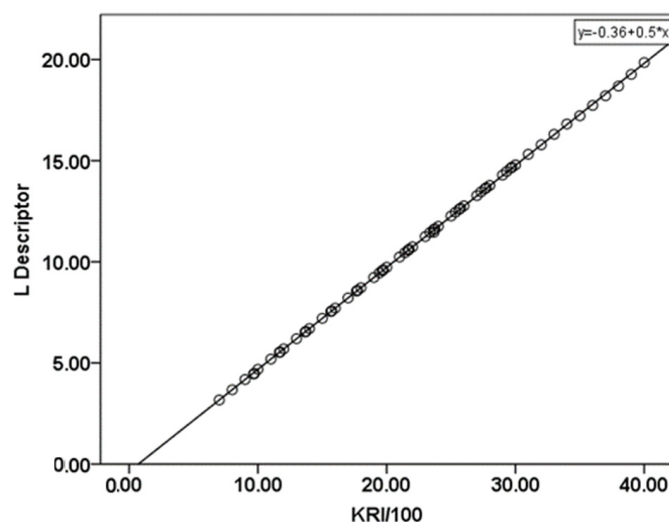

Figure 1. Graphical plot of the **L** solute descriptors versus ($KRI/100$) data for the 63 compounds used in the least-squares regression analysis for obtaining Equation (5).

3. Calculation of Thermodynamic Properties of Large Methylated Alkanes Using Abraham Model Solute Descriptors

The **L** solute descriptors that are tabulated in the last column of Table 1 provide researchers with an additional 149 chemical compounds to use in developing group contribution and machine learning methods for predicting Abraham model solute descriptors. Remember that the **E**, **S**, **A** and **B** solute descriptors of the tabulated compounds are equal to zero, and that the **V** solute descriptor values can be easily obtained using the method described by Abraham and McGowan [73]. The tabulated values given in Table 1 can also be used in conjunction with published Abraham model correlations to predict a wide range of physical, biological and thermodynamic properties including vapor pressures, enthalpies of vaporization and sublimation, enthalpies of solvation, aquatic toxicities and other properties. In the next few paragraphs, we will illustrate the computational methodology by calculating the standard molar enthalpies of sublimation, $\Delta H_{\text{sub,298K}}$, and of vaporization at 298 K, $\Delta H_{\text{vap,298K}}$, as well as discussing how the former values might be combined with measured enthalpy of solution data, $\Delta H_{\text{soln,298K}}$, to obtain a second set of predicted $\Delta H_{\text{sub,298K}}$ values. While our computations are focused on the large, methylated alkanes studied in the current communication, we note that the computational method can be applied to other organic compounds as well. All that is needed for the predictions is knowledge of the Abraham model solute descriptors for the given compound and the Abraham model correlation for the property/process that one wishes to predict. This is the driving force behind the development of group contribution and machine learning methods to predict Abraham model solute descriptors.

For the methylated alkane compounds studied in the current communication, the numerical values of $\Delta H_{\text{sub,298K}}$ are calculated according to Equation (6) [46].

$$\Delta H_{\text{sub,298K}} = 13.93 + 13.57 \, \mathbf{L} - 0.05 \, \mathbf{L} \times \mathbf{L} \tag{6}$$

For the convenience of the journal readers, we have removed the $e_k \times \mathbf{E}$, $s_k \times \mathbf{S}$, $a_k \times \mathbf{A}$ and $b_k \times \mathbf{B}$ terms from Equation (2) as these terms will not contribute to the calculated $\Delta H_{\text{sub,298K}}$ values because the $\mathbf{E}$, $\mathbf{S}$, $\mathbf{A}$ and $\mathbf{B}$ solute descriptors of the methylated alkane compounds are set equal to zero. The second column in Table 2 contains our calculated $\Delta H_{\text{sub,298K}}$ values for the 178 compounds gathered from the Katritzky et al. [72] paper.

Table 2. Comparison of the enthalpies of sublimation, $\Delta H_{\text{sub,298K}}$ (in kJ mol^{-1}), predicted by the Abraham model Equation (6) and the group-additivity method of Naef and Acree (Equation (8)).

Compound Name	$\Delta H_{\text{sub,298K}}$ Equation (6)	$\Delta H_{\text{sub,298K}}$ Equation (8)
Monomethylalkanes		
2-Methylnonane	73.4	77.3
3-Methylnonane	73.8	77.3
2-Methylundecane	87.3	90.0
3-Methylundecane	87.7	90.0
2-Methyltridecane	100.4	102.7
3-Methyltridecane	100.8	102.7
2-Methylpentadecane	113.4	115.4
3-Methylpentadecane	113.9	115.4
2-Methylheptadecane	126.3	128.1
3-Methylheptadecane	126.8	128.1
2-Methylnonadecane	139.1	140.8
3-Methylnonadecane	139.7	140.8
10-Methylnonadecane	137.7	140.8
2-Methylheneicosane	151.8	153.5
3-Methylheneicosane	152.4	153.5
11-Methylheneicosane	150.3	153.5
2-Methyltricosane	164.4	166.2
3-Methyltricosane	165.1	166.2
8-Methyltricosane	163.0	166.2
12-Methyltricosane	162.7	166.2
2-Methylpentacosane	177.0	178.9
3-Methylpentacosane	177.6	178.9
13-Methylpentacosane	175.2	178.9
2-Methylheptacosane	189.4	191.6
3-Methylheptacosane	190.0	191.6
14-Methylheptacosane	187.5	191.6
2-Methylnonacosane	201.7	204.3
3-Methylnonacosane	202.4	204.3
15-Methylnonacosane	199.8	204.3
2-Methylhentriacontane	213.2	217.0
3-Methylhentriacontane	214.0	217.0
4-Methylhentriacontane	213.0	217.0
5-Methylhentriacontane	212.5	217.0
6-Methylhentriacontane	212.1	217.0
7-Methylhentriacontane	211.9	217.0
13-Methylhentriacontane	211.3	217.0
16-Methylhentriacontane	211.3	217.0
2-Methyltritriacontane	225.3	229.7
3-Methyltritriacontane	226.0	229.7
4-Methyltritriacontane	225.0	229.7
5-Methyltritriacontane	224.6	229.7
6-Methyltritriacontane	224.2	229.7
13-Methyltritriacontane	223.3	229.7
17-Methyltritriacontane	223.3	229.7
2-Methylpentatriacontane	237.2	242.4
3-Methylpentatriacontane	238.0	242.4
18-Methylpentatriacontane	235.2	242.4

Table 2. *Cont.*

Compound Name	$\Delta H_{sub,298K}$ Equation (6)	$\Delta H_{sub,298K}$ Equation (8)
Dimethylalkanes		
3,9-Dimethyltricosane	167.0	167.0
5,9-Dimethyltetracosane	171.7	173.4
3,11-Dimethylpentacosane	179.4	179.7
3,15-Dimethylpentacosane	179.1	179.7
5,11-Dimethylpentacosane	177.7	179.7
5,17-Dimethylpentacosane	177.9	179.7
7,11-Dimethylpentacosane	177.4	179.7
2,6-Dimethylhexacosane	185.2	186.1
4,8-Dimethylhexacosane	184.7	186.1
5,11-Dimethylhexacosane	183.9	186.1
6,10-Dimethylhexacosane	183.6	186.1
7,11-Dimethylhexacosane	183.4	186.1
3,7-Dimethylheptacosane	191.7	192.4
3,15-Dimethylheptacosane	191.4	192.4
5,11-Dimethylheptacosane	190.0	192.4
5,17-Dimethylheptacosane	190.3	192.4
7,13-Dimethylheptacosane	189.5	192.4
9,19-Dimethylheptacosane	189.0	192.4
2,6-Dimethyloctacosane	197.6	198.8
2,10-Dimethyloctacosane	197.2	198.8
4,10-Dimethyloctacosane	197.0	198.8
5,15-Dimethyloctacosane	196.2	198.8
7,13-Dimethyloctacosane	195.6	198.8
3,7-Dimethylnonacosane	203.9	205.1
3,13-Dimethylnonacosane	203.6	205.1
5,13-Dimethylnonacosane	202.3	205.1
5,19-Dimethylnonacosane	202.3	205.1
7,17-Dimethylnonacosane	201.7	205.1
2,6-Dimethyltriacontane	209.8	211.5
2,10-Dimethyltriacontane	209.4	211.5
2,12-Dimethyltriacontane	209.2	211.5
3,7-Dimethyltriacontane	210.0	211.5
4,10-Dimethyltriacontane	209.1	211.5
6,10-Dimethyltriacontane	207.9	211.5
3,7-Dimethylhentriacontane	216.1	217.8
3,13-Dimethylhentriacontane	215.7	217.8
3,15-Dimethylhentriacontane	216.1	217.8
5,13-Dimethylhentriacontane	214.3	217.8
5,17-Dimethylhentriacontane	214.4	217.8
7,11-Dimethylhentriacontane	213.7	217.8
11,21-Dimethylhentriacontane	213.3	217.8
2,8-Dimethyldotriacontane	221.4	224.2
4,8-Dimethyldotriacontane	221.1	224.2
6,10-Dimethyldotriacontane	219.9	224.2
8,12-Dimethyldotriacontane	219.5	224.2
9,21-Dimethyldotriacontane	219.3	224.2
14,18-Dimethyldotriacontane	219.0	224.2
3,9-Dimethyltritriacontane	227.7	230.5
3,15-Dimethyltritriacontane	228.1	230.5
5,16-Dimethyltritriacontane	226.4	230.5
5,19-Dimethyltritriacontane	226.5	230.5
7,17-Dimethyltritriacontane	225.8	230.5
11,23-Dimethyltritriacontane	225.3	230.5
2,10-Dimethyltetratriacontane	233.2	236.9
4,16-Dimethyltetratriacontane	232.9	236.9
6,10-Dimethyltetratriacontane	232.0	236.9
8,12-Dimethyltetratriacontane	231.5	236.9
12,22-Dimethyltetratriacontane	231.2	236.9

Table 2. *Cont.*

Compound Name	$\Delta H_{sub,298K}$ Equation (6)	$\Delta H_{sub,298K}$ Equation (8)
13,17-Dimethyltetratriacontane	230.9	236.9
3,7-Dimethylpentatriacontane	240.1	243.2
3,15-Dimethylpentatriacontane	239.6	243.2
5,9-Dimethylpentatriacontane	238.3	243.2
5,19-Dimethylpentatriacontane	238.3	243.2
7,17-Dimethylpentatriacontane	237.7	243.2
9,21-Dimethylpentatriacontane	237.2	243.2
2,12-Dimethylhexatriacontane	245.1	249.6
5,17-Dimethylhexatriacontane	244.2	249.6
13,23-Dimethylhexatriacontane	243.1	249.6
3,15-Dimethylheptatriacontane	251.4	255.9
5,19-Dimethylheptatriacontane	250.1	255.9
5,17-Dimethylheptatriacontane	250.2	255.9
13,23-Dimethylheptatriacontane	248.9	255.9
5,17-Dimethyloctatriacontane	255.9	262.3
Trimethylalkanes		
4,8,12-Trimethyltetracosane	173.8	174.2
5,9,13-Trimethylpentacosane	179.4	180.6
4,8,12-Trimethylhexacosane	186.2	186.9
3,7,11-Trimethylheptacosane	193.5	193.3
4,8,12-Trimethyloctacosane	198.4	199.6
3,7,11-Trimethylnonacosane	205.6	206.0
5,13,17-Trimethylnonacosane	203.8	206.0
6,14,18-Trimethyltriacontane	209.5	212.3
3,7,11-Trimethylhentriacontane	217.7	218.7
5,13,17-Trimethylhentriacontane	215.8	218.7
7,13,17-Trimethylhentriacontane	215.0	218.7
11,15,19-Trimethylhentriacontane	214.4	218.7
2,10,16-Trimethyldotriacontane	223.0	225.0
4,12,16-Trimethyldotriacontane	222.5	225.0
6,14,18-Trimethyldotriacontane	221.5	225.0
12,16,20-Trimethyldotriacontane	220.4	225.0
3,7,15-Trimethyltritriacontane	229.7	231.4
5,13,17-Trimethyltritriacontane	227.9	231.4
7,11,15-Trimethyltritriacontane	226.9	231.4
11,15,19-Trimethyltritriacontane	226.3	231.4
2,10,16-Trimethyltetratriacontane	235.0	237.7
4,8,12-Trimethyltetratriacontane	234.5	237.7
6,14,18-Trimethyltetratriacontane	233.4	237.7
8,12,16-Trimethyltetratriacontane	232.7	237.7
12,16,20-Trimethyltetratriacontane	232.2	237.7
3,7,15-Trimethylpentatriacontane	241.7	244.1
5,9,13-Trimethylpentatriacontane	239.8	244.1
7,11,15-Trimethylpentatriacontane	238.8	244.1
13,17,21-Trimethylpentatriacontane	238.1	244.1
13,17,23-Trimethylpentatriacontane	238.5	244.1
4,8,16-Trimethylhexatriacontane	246.3	250.4
8,12,16-Trimethylhexatriacontane	244.5	250.4
14,18,22-Trimethylhexatriacontane	244.0	250.4
3,7,15-Trimethylheptatriacontane	253.4	256.8
5,13,17-Trimethylheptatriacontane	251.5	256.8
7,13,19-Trimethylheptatriacontane	250.4	256.8
15,19,23-Trimethylheptatriacontane	249.9	256.8
15,19,23-Trimethyloctatriacontane	255.7	263.1
5,13,17-Trimethylnonatriacontane	263.1	269.5
15,19,23-Trimethylnonatriacontane	261.5	269.5
14,18,22-Trimethyltetracontane	267.2	275.8

Table 2. *Cont.*

Compound Name	$\Delta H_{sub,298K}$ Equation (6)	$\Delta H_{sub,298K}$ Equation (8)
Tetramethylalkanes		
3,7,11,15-Tetramethylnonacosane	207.2	206.8
3,7,11,15-Tetramethylhentriacontane	219.2	219.5
4,8,12,16-Tetramethylhentriacontane	218.5	219.5
3,7,11,15-Tetramethyltritriacontane	231.1	232.2
4,8,12,16-Tetramethyltritriacontane	230.4	232.2
3,7,11,15-Tetramethylpentatriacontane	242.9	244.9
7,11,15,19-Tetramethylpentatriacontane	241.2	244.9
9,13,17,21-Tetramethylpentatriacontane	240.5	244.9
11,15,19,24-Tetramethylpentatriacontane	239.8	244.9
6,10,12,16-Tetramethylhexatriacontane	246.8	251.3
8,12,16,20-Tetramethylhexatriacontane	246.2	251.3
10,14,18,22-Tetramethylhexatriacontane	245.6	251.3
3,7,11,15-Tetramethylheptatriacontane	254.6	257.6
7,11,15,19-Tetramethylheptatriacontane	252.7	257.6
9,13,17,21-Tetramethylheptatriacontane	252.1	257.6
11,15,19,24-Tetramethylheptatriacontane	251.5	257.6
10,14,18,22-Tetramethyloctatriacontane	257.2	264.0

In our search of the published chemical and engineering literature we did not find experimental $\Delta H_{sub,298K}$ data to compare our calculated values against. The sublimation enthalpies of large, nonvolatile compounds are difficult to measure due to the compound's very small vapor pressures; however, these quantities are often needed in the design of high-temperature industrial processes and in the calculation of gas-phase standard molar enthalpies of formation from enthalpy of combustion measurements. What we offer in the way of a comparison is to compare our Abraham model predictions against the calculated values from the Naef and Acree group-additivity method [14]. The group-additivity method has been shown to predict $\Delta H_{sub,298K}$ values for approximately 1866 molecular compounds to within a standard deviation of $SD = 10.33$ kJ mol^{-1}. The basic method estimates a given thermodynamic or physical property by:

$$Property = \sum_i A_i a_i + \sum_j B_j b_j + Constant \tag{7}$$

summing the contributions that each individual atom group makes to the overall property. In Equation (7), A_i denotes the number of occurrences of the ith atom group, B_j is the number of times each special group occurs, and a_i and b_j are the numerical values of each atom group and special group.

For monomethylated and polymethylated alkanes, the atom group-additivity method proposed by Naef and Acree [14] fragments molecules into three distinct kinds of sp^3 hybridized carbon atoms based on the number of each type of atoms directly bonded to the carbon atom. The first carbon-atom group will be bonded to three hydrogen atoms and one carbon atom (CH$_3$ group), the second carbon-atom group will be attached to two hydrogen and two carbon atoms (CH$_2$ group), and the third carbon-atom group has a single hydrogen and three carbon-atom nearest neighbors (CH group). The method also includes one special group that is defined as the total number of carbon atoms in the alkane molecule.

In Equation (8) below we have inserted the numerical group values and constants into Equation (7) for predicting $\Delta H_{sub,298K}$ of C_nH_{2n+2} monomethylated and polymethylated alkanes:

$$\Delta H_{sub,298K} \text{ (kJ mol}^{-1}) = 5.99\, n_{CH3} + 6.88\, n_{CH2} + 2.28\, n_{CH} - 0.53\, n_{carbons} + 21.03 \tag{8}$$

We note that the predicted values based on Equation (6) of the Abraham model are similar to the predictions based on the group-additivity model of Naef and Acree [14] for the "smaller" of the large polymethylated alkanes as shown by the numerical entries in

the last two columns of Table 2. The differences become more pronounced with increasing carbon-atom chain length. The group-additivity method is unable to distinguish between the placement of the alkyl-substituent group along the large carbon-atom chain, and yields the same predicted values for a common set of number of different atom types. In other words, the predicted values of all dimethylhexacosane isomers in Table 2 are the same. Every dimethylhexacosane isomer considered in this study has 4 CH_3-type carbon atoms, 22 CH_2-type carbon atoms, 2 CH-type carbon atoms, and 28 total carbon atoms. The only dimethylhexacosane isomers that would be different would be those in which both methyl groups were situated on the same carbon atom. The predicted values of these latter dimethylhexacosane isomers would be identical to each other, but different from the dimethylhexacosane isomers in Table 2. Identical predicted values for isomeric compounds are a common feature of most published group-additivity and group contribution methods for predicting thermodynamic properties of organic compounds. The Abraham model, on the other hand, will give different predicted values for each dimethylhexacosane isomer, and does not require that the molecule be fragmented into atom groups or functional groups.

The enthalpies of vaporization would be calculated in similar fashion using the mathematical correlation developed by Churchill and coworkers [45]:

$$\Delta H_{vap,298K} \text{ (kJ mol}^{-1}) = 6.100 + 9.537 \text{ } \mathbf{L} \tag{9}$$

and the group-additivity method proposed by Naef and Acree [14]:

$$\Delta H_{vap,298K} \text{ (kJ mol}^{-1}) = 3.07 \text{ } n_{CH3} + 4.67 \text{ } n_{CH2} + 3.57 \text{ } n_{CH} + 0.09 \text{ } n_{carbons} + 8.61 \tag{10}$$

As before, only the terms needed in the calculation of the $\Delta H_{vap,298K}$ values for the polymethylated alkanes studied in the current communication are given. The standard molar enthalpies of vaporization of large alkanes can be experimentally determined using correlation gas chromatography [74–76]. The experimental method is applicable to both solid and liquid compounds, and moreover, does not require highly purified chemical samples as the chromatographic retention times corresponding to the dissolved impurities in the samples can be distinguished from the desired chemical compound by their much smaller peak areas.

Solomonov and coworkers [77–81] recently devised an indirect method for determining both standard molar enthalpies of vaporization and sublimation from measured enthalpies of solution, ΔH_{soln}, and predicted enthalpies of solvation, ΔH_{solv}, for the given chemical compound dissolved in a suitable organic solvent. Numerical values of $\Delta H_{vap,298K}$ and $\Delta H_{sub,298K}$ were calculated from:

$$\Delta H_{vap,298K} = \Delta H_{soln,298K} - \Delta H_{solv,298K} \tag{11}$$

$$\Delta H_{sub,298K} = \Delta H_{soln,298K} - \Delta H_{solv,298K} \tag{12}$$

Equations (11) and (12), respectively, depending upon whether the dissolved solute is a liquid or crystalline compound. The standard molar vaporization/sublimation enthalpies of vaporization and sublimation based upon the proposed solution calorimetry approach of Solomonov and coworkers were found to be in good agreement (within experimental uncertainties) with the values determined by the more direct calorimetric, gas saturation and vapor pressure methods. The Abraham general solvation model was one of the predictive methods used by the authors [81] to calculate the solvation enthalpies. Abraham model correlations are available for calculating ΔH_{solv}, values for solutes dissolved in water and in more than 30 different organic solvents of varying polarity and hydrogen-bonding character. Group contribution and atom-additivity methods for predicting enthalpies of solvation are currently available for only a handful of organic solvents. In Table 3 we have

tabulated the ΔH_{solv} values for 178 different polymethylated alkanes dissolved in benzene based upon:

$$\Delta H_{\text{solv,298K}} \text{ (kJ mol}^{-1}) = -5.175(0.354) - 8.393(0.103) \textbf{ L} \qquad (13)$$

the updated Abraham model correlation reported by Lu et al. [82] The above correlation contains only the terms needed to predict values for the compounds studied in the current communication.

Table 3. Predicted gas-to-benzene enthalpies of solvation, $\Delta H_{\text{solv,298K}}$ (in kJ mol^{-1}) for 178 monomethylated and polymethylated alkanes based upon Equation (13).

Compound Name	$\Delta H_{\text{solv,298K}}$ (kJ mol^{-1})	Compound Name	$\Delta H_{\text{solv,298K}}$ (kJ mol^{-1})
Monomethylalkanes		**Dimethylalkanes**	
2-Methylnonane	−42.6	3,9-Dimethyltricosane	−104.1
3-Methylnonane	−42.8	5,9-Dimethyltetracosane	−107.3
2-Methylundecane	−51.5	3,11-Dimethylpentacosane	−112.6
3-Methylundecane	−51.8	3,15-Dimethylpentacosane	−112.4
2-Methyltridecane	−60.0	5,11-Dimethylpentacosane	−111.4
3-Methyltridecane	−60.3	5,17-Dimethylpentacosane	−111.5
2-Methylpentadecane	−68.5	7,11-Dimethylpentacosane	−111.2
3-Methylpentadecane	−68.8	2,6-Dimethylhexacosane	−116.6
2-Methylheptadecane	−76.9	4,8-Dimethylhexacosane	−116.2
3-Methylheptadecane	−77.3	5,11-Dimethylhexacosane	−115.6
2-Methylnonadecane	−85.4	6,10-Dimethylhexacosane	−115.5
3-Methylnonadecane	−85.8	7,11-Dimethylhexacosane	−115.3
10-Methylnonadecane	−84.5	3,7-Dimethylheptacosane	−121.0
2-Methylheneicosane	−93.9	3,15-Dimethylheptacosane	−120.8
3-Methylheneicosane	−94.3	5,11-Dimethylheptacosane	−119.9
11-Methylheneicosane	−92.9	5,17-Dimethylheptacosane	−120.0
2-Methyltricosane	−102.4	7,13-Dimethylheptacosane	−119.5
3-Methyltricosane	−102.8	9,19-Dimethylheptacosane	−119.2
8-Methyltricosane	−101.4	2,6-Dimethyloctacosane	−125.1
12-Methyltricosane	−101.3	2,10-Dimethyloctacosane	−124.8
2-Methylpentacosane	−110.9	4,10-Dimethyloctacosane	−124.7
3-Methylpentacosane	−111.4	5,15-Dimethyloctacosane	−124.1
13-Methylpentacosane	−109.7	7,13-Dimethyloctacosane	−123.7
2-Methylheptacosane	−119.4	3,7-Dimethylnonacosane	−129.4
3-Methylheptacosane	−119.9	3,13-Dimethylnonacosane	−129.3
14-Methylheptacosane	−118.1	5,13-Dimethylnonacosane	−128.3
2-Methylnonacosane	−127.9	5,19-Dimethylnonacosane	−128.4
3-Methylnonacosane	−128.4	7,17-Dimethylnonacosane	−128.0
15-Methylnonacosane	−126.6	2,6-Dimethyltriacontane	−133.5
2-Methylhentriacontane	−135.9	2,10-Dimethyltriacontane	−133.3
3-Methylhentriacontane	−136.5	2,12-Dimethyltriacontane	−133.1
4-Methylhentriacontane	−135.8	3,7-Dimethyltriacontane	−133.7
5-Methylhentriacontane	−135.4	4,10-Dimethyltriacontane	−133.1
6-Methylhentriacontane	−135.2	6,10-Dimethyltriacontane	−132.3
7-Methylhentriacontane	−135.0	3,7-Dimethylhentriacontane	−137.9
13-Methylhentriacontane	−134.6	3,13-Dimethylhentriacontane	−137.7
16-Methylhentriacontane	−134.6	3,15-Dimethylhentriacontane	−137.9
2-Methyltritriacontane	−144.4	5,13-Dimethylhentriacontane	−136.7
3-Methyltritriacontane	−144.9	5,17-Dimethylhentriacontane	−136.8
4-Methyltritriacontane	−144.2	7,11-Dimethylhentriacontane	−136.3
5-Methyltritriacontane	−143.9	11,21-Dimethylhentriacontane	−136.0
6-Methyltritriacontane	−143.6	2,8-Dimethyldotriacontane	−141.7
13-Methyltritriacontane	−143.0	4,8-Dimethyldotriacontane	−141.4
17-Methyltritriacontane	−143.0	6,10-Dimethyldotriacontane	−140.6
2-Methylpentatriacontane	−152.9	8,12-Dimethyldotriacontane	−140.3
3-Methylpentatriacontane	−153.4	9,21-Dimethyldotriacontane	−140.2
18-Methylpentatriacontane	−151.4	14,18-Dimethyldotriacontane	−140.0

Table 3. *Cont.*

Compound Name	$\Delta H_{solv,298K}$ (kJ mol^{-1})	Compound Name	$\Delta H_{solv,298K}$ (kJ mol^{-1})
Trimethylalkane		3,9-Dimethyltritriacontane	−146.1
4,8,12-Trimethyltetracosane	−108.8	3,15-Dimethyltritriacontane	−146.4
5,9,13-Trimethylpentacosane	−112.6	5,16-Dimethyltritriacontane	−145.2
4,8,12-Trimethylhexacosane	−117.2	5,19-Dimethyltritriacontane	−145.3
3,7,11-Trimethylheptacosane	−122.2	7,17-Dimethyltritriacontane	−144.7
4,8,12-Trimethyloctacosane	−125.6	11,23-Dimethyltritriacontane	−144.4
3,7,11-Trimethylnonacosane	−130.7	2,10-Dimethyltetratriacontane	−150.0
5,13,17-Trimethylnonacosane	−129.4	4,16-Dimethyltetratriacontane	−149.8
6,14,18-Trimethyltriacontane	−133.3	6,10-Dimethyltetratriacontane	−149.1
3,7,11-Trimethylhentriacontane	−139.1	8,12-Dimethyltetratriacontane	−148.8
5,13,17-Trimethylhentriacontane	−137.8	12,22-Dimethyltetratriacontane	−148.6
7,13,17-Trimethylhentriacontane	−137.2	13,17-Dimethyltetratriacontane	−148.3
11,15,19-Trimethylhentriacontane	−136.8	3,7-Dimethylpentatriacontane	−154.9
2,10,16-Trimethyldotriacontane	−142.8	3,15-Dimethylpentatriacontane	−154.5
4,12,16-Trimethyldotriacontane	−142.5	5,9-Dimethylpentatriacontane	−153.6
6,14,18-Trimethyldotriacontane	−141.7	5,19-Dimethylpentatriacontane	−153.6
12,16,20-Trimethyldotriacontane	−141.0	7,17-Dimethylpentatriacontane	−153.2
3,7,15-Trimethyltritriacontane	−147.6	9,21-Dimethylpentatriacontane	−152.8
5,13,17-Trimethyltritriacontane	−146.2	2,12-Dimethylhexatriacontane	−158.5
7,11,15-Trimethyltritriacontane	−145.5	5,17-Dimethylhexatriacontane	−157.9
11,15,19-Trimethyltritriacontane	−145.2	13,23-Dimethylhexatriacontane	−157.1
2,10,16-Trimethyltetratricontane	−151.3	3,15-Dimethylheptatriacontane	−163.0
4,8,12-Trimethyltetratriacontane	−150.9	5,19-Dimethylheptatriacontane	−162.0
6,14,18-Trimethyltetratriacontane	−150.1	5,17-Dimethylheptatriacontane	−162.1
8,12,16-Trimethyltetratriacontane	−149.7	13,23-Dimethylheptatriacontane	−161.2
12,16,20-Trimethyltetratriacontane	−149.3	5,17-Dimethyloctatriacontane	−166.2
3,7,15-Trimethylpentatriacontane	−156.0	**Tetramethylalkane**	
5,9,13-Trimethylpentatriacontane	−154.7	3,7,11,15-Tetramethylnonacosane	−131.7
7,11,15-Trimethylpentatriacontane	−154.0	3,7,11,15-Tetramethylhentriacontane	−140.1
13,17,21-Trimethylpentatriacontane	−153.5	4,8,12,16-Tetramethylhentriacontane	−139.6
13,17,23-Trimethylpentatriacontane	−153.8	3,7,11,15-Tetramethyltritriacontane	−148.5
4,8,16-Trimethylhexatriacontane	−159.3	4,8,12,16-Tetramethyltritriacontane	−148.0
8,12,16-Trimethylhexatriacontane	−158.1	3,7,11,15-Tetramethylpentatriacontane	−156.9
14,18,22-Trimethylhexatriacontane	−157.7	7,11,15,19-Tetramethylpentatriacontane	−155.7
3,7,15-Trimethylheptatriacontane	−164.4	9,13,17,21-Tetramethylpentatriacontane	−155.2
5,13,17-Trimethylheptatriacontane	−163.1	11,15,19,24-Tetramethylpentatriacontane	−154.7
7,13,19-Trimethylheptatriacontane	−162.3	6,10,12,16-Tetramethylhexatriacontane	−159.8
15,19,23-Trimethylheptatriacontane	−161.9	8,12,16,20-Tetramethylhexatriacontane	−159.3
15,19,23-Trimethyloctatriacontane	−166.0	10,14,18,22-Tetramethylhexatriacontane	−158.9
5,13,17-Trimethylnonatriacontane	−171.4	3,7,11,15-Tetramethylheptatriacontane	−165.3
15,19,23-Trimethylnonatriacontane	−170.2	7,11,15,19-Tetramethylheptatriacontane	−163.9
14,18,22-Trimethyltetracontane	−174.4	9,13,17,21-Tetramethylheptatriacontane	−163.5
		11,15,19,24-Tetramethylheptatriacontane	−163.1
		10,14,18,22-Tetramethyloctatriacontane	−167.2

4. Conclusions

The current study is a continuation of our ongoing research involving the calculation Abraham model solute descriptors based on experimental water-to-organic solvent partition coefficients, infinite dilution activity coefficients, molar solubilities and gas–liquid chromatographic and high-performance liquid chromatographic retention data. Abraham model **L** solute descriptors have been calculated for an additional 149 C$_{11}$ to C$_{42}$ monomethylated and polymethylated alkanes based on the measured Kovat's gas–liquid chromatographic retention indices retrieved from the published chemical literature. The calculated solute descriptors, in combination with previously published Abraham model correlations, can be used to predict a number of very important chemical and thermodynamic properties including partition coefficients, molar solubility ratios, gas–liquid

chromatographic and HPLC retention data, infinite dilution activity coefficients, molar enthalpies of solvation, standard molar vaporization and sublimation at 298 K, vapor pressures, and limiting diffusion coefficients. The predictive computations are illustrated by estimating both the standard molar enthalpies of sublimation and the enthalpies of solvation in benzene for the monomethylated and polymethylated alkanes considered in the current study. The standard molar enthalpy of sublimation predictions were also performed using the group-additivity method proposed by Naef and Acree. Experimental thermodynamic data are not currently available for many of the larger monomethylated and polymethylated alkanes. Predictive methods provide practicing chemists and engineers working in the industrial manufacturing sector with a means to estimate the physical and thermodynamic properties needed in process design calculations.

A comparison of the two methods revealed that the $\Delta H_{sub,298K}$ predictions based on the Abraham model are similar to predictions based on the group-additivity model of Naef and Acree [14] for the "smaller" of the large polymethylated alkanes. The differences became more pronounced with increasing carbon-atom chain length. The group-additivity method was not able to distinguish between the placement of the alkyl-substituent group attached to the large carbon-atom chain, and yielded the same predicted values for a given molecular formula. In other words, the predicted values of all dimethylhexacosane isomers were the same. This limitation is a common feature of most group-additivity and group contribution methods. The Abraham model, on the other hand, provides different predicted values for the different dimethylhexacosane molecules, and does not require fragmentation of the molecule into atom groups or functional groups.

The solute descriptors determined in the current study further the development of group contribution and machine learning methods by providing experimental-based values for an additional 149 chemical compounds. Published group contribution [53–56] and machine learning methods [55,56] have shown some promise along these lines in that the estimated descriptor values provide reasonably accurate predictions for both the molar enthalpies of solvation (ΔH_{solv}) and molar Gibbs energies of solvation (ΔG_{solv}) of organic solutes and inorganic gases in a wide range of organic solvents of varying polarity and hydrogen-bonding character.

References

1. Ruddigkeit, L.; van Deursen, R.; Blum, L.C.; Reymond, J.-L. Enumeration of 166 billion organic small molecules in the Chemical Universe Database GDB-17. *J. Chem. Inf. Model.* **2012**, *52*, 2864–2875. [CrossRef] [PubMed]
2. Toots, K.M.; Sild, S.; Leis, J.; Acree, W.E., Jr.; Maran, U. The quantitative structure-property relationships for the gas-ionic liquid partition coefficient of a large variety of organic compounds in three ionic liquids. *J. Mol. Liq.* **2021**, *343*, 117573. [CrossRef]
3. Katritzky, A.R.; Oliferenko, A.A.; Oliferenko, P.V.; Petrukhin, R.; Tatham, D.B.; Maran, U.; Lomaka, A.; Acree, W.E., Jr. A general treatment of solubility. 1. The QSPR correlation of solvation free energies of single solutes in series of solvents. *J. Chem. Inf. Comp. Sci.* **2003**, *43*, 1794–1805. [CrossRef] [PubMed]

4.   Katritzky, A.R.; Oliferenko, A.A.; Oliferenko, P.V.; Petrukhin, R.; Tatham, D.B.; Maran, U.; Lomaka, A.; Acree, W.E., Jr. A general treatment of solubility. 2. QSPR prediction of free energies of solvation of specified solutes in ranges of solvents. *J. Chem. Inf. Comp. Sci.* **2003**, *43*, 1806–1814. [CrossRef] [PubMed]

5.   Shang, Z.C.; Zou, J.W.; Huang, M.L.; Yu, Q.S. QSPR studies on solubilities of some given solutes in pure solvents using frontier orbital energies and theoretical descriptors derived from electrostatic potentials on molecular surface. *Acta Chim. Sin.* **2002**, *60*, 647–652.

6.   Golmohammadi, H.; Dashtbozorgi, Z.; Gholam Samani, M.; Acree, W.E., Jr. QSPR prediction of gas-to-methanol solvation enthalpy of organic compounds using replacement method and support vector machine. *Phys. Chem. Liq.* **2015**, *53*, 46–66. [CrossRef]

7.   Sola, D.; Ferri, A.; Banchero, M.; Manna, L.; Sicardi, S. QSPR prediction of N-boiling point and critical properties of organic compounds and comparison with a group-contribution method. *Fluid Phase Equilib.* **2008**, *263*, 33–42. [CrossRef]

8.   Zhou, L.; Wang, B.; Jiang, J.; Pan, Y.; Wang, Q. Quantitative structure-property relationship (QSPR) study for predicting gas-liquid critical temperatures of organic compounds. *Thermochim. Acta* **2017**, *655*, 112–116. [CrossRef]

9.   Naef, R.; Acree, W.E., Jr. Revision and extension of a generally applicable group-additivity method for the calculation of the standard heat of combustion and formation of organic molecules. *Molecules* **2021**, *26*, 6101. [CrossRef]

10.   Naef, R.; Acree, W.E., Jr. Calculation of the surface tension of ordinary organic and ionic liquids by means of a generally applicable computer algorithm based on the group-additivity method. *Molecules* **2018**, *23*, 1224. [CrossRef]

11.   Naef, R.; Acree, W.E., Jr. Application of a general computer algorithm based on the group-additivity method for the calculation of two molecular descriptors at both ends of dilution: Liquid viscosity and activity coefficient in water at infinite dilution. *Molecules* **2018**, *23*, 5. [CrossRef] [PubMed]

12.   Naef, R.; Acree, W.E., Jr. Calculation of the vapour pressure of organic molecules by means of a group-additivity method and their resultant Gibbs free energy and entropy of vaporization at 298.15 K. *Molecules* **2021**, *26*, 1045. [CrossRef]

13.   Naef, R. A generally applicable computer algorithm based on the group additivity method for the calculation of seven molecular descriptors: Heat of combustion, Log $P_{O/W}$, Log S, refractivity, polarizability, toxicity and Log BB of organic compounds; scope and limits of applicability. *Molecules* **2015**, *20*, 18279–18351. [PubMed]

14.   Naef, R.; Acree, W.E., Jr. Calculation of five thermodynamic molecular descriptors by means of a general computer algorithm based on the group-additivity method: Standard enthalpies of vaporization, sublimation and solvation, and entropy of fusion of ordinary organic molecules and total phase-change entropy of liquid crystals. *Molecules* **2017**, *22*, 1059.

15.   Gharagheizi, F.; Ilani-Kashkouli, P.; Acree, W.E., Jr.; Mohammadi, A.H.; Ramjugernath, D. A group contribution model for determining the sublimation enthalpy of organic compounds at the standard reference temperature of 298 K. *Fluid Phase Equilib.* **2013**, *354*, 265–285. [CrossRef]

16.   Gharagheizi, F.; Ilani-Kashkouli, P.; Acree, W.E., Jr.; Mohammadi, A.H.; Ramjugernath, D. A group contribution model for determining the vaporization enthalpy of organic compounds at the standard reference temperature of 298 K. *Fluid Phase Equilib.* **2013**, *360*, 279–292. [CrossRef]

17.   Abraham, M.H. Scales of solute hydrogen-bonding: Their construction and application to physicochemical and biochemical processes. *Chem. Soc. Rev.* **1993**, *22*, 73–83. [CrossRef]

18.   Abraham, M.H.; Ibrahim, A.; Zissimos, A.M. Determination of sets of solute descriptors from chromatographic measurements. *J. Chromatogr. A* **2004**, *1037*, 29–47. [CrossRef]

19.   Abraham, M.H.; Smith, R.E.; Luchtefeld, R.; Boorem, A.J.; Luo, R.; Acree, W.E., Jr. Prediction of solubility of drugs and other compounds in organic solvents. *J. Pharm. Sci.* **2010**, *99*, 1500–1515. [CrossRef]

20.   Abraham, M.H.; Acree, W.E., Jr. Descriptors for the prediction of partition coefficients of 8-hydroxyquinoline and its derivatives. *Sep. Sci. Technol.* **2014**, *49*, 2135–2141. [CrossRef]

21.   Smart, K.; Connolly, E.; Ocon, L.; Golden, T.; Acree, W.E.; Abraham, M.H. Abraham model correlations for describing the partition of organic compounds from water into the methyl ethyl ketone extraction solvent. *Phys. Chem. Liq.* **2022**, *60*, 47–58. [CrossRef]

22.   Smart, K.; Garcia, E.; Oloyede, B.; Fischer, R.; Golden, T.D.; Acree, W.E., Jr.; Abraham, M.H. The partition of organic compounds from water into the methyl isobutyl ketone extraction solvent with updated Abraham model equation. *Phys. Chem. Liq.* **2021**, *59*, 431–441. [CrossRef]

23.   Liu, X.; Acree, W.E., Jr.; Abraham, M.H. Descriptors for some compounds with pharmacological activity; calculation of properties. *Int. J. Pharm.* **2022**, *617*, 121597. [CrossRef] [PubMed]

24.   Abraham, M.H.; Acree, W.E., Jr.; Brumfield, M.; Hart, E.; Pipersburgh, L.; Mateja, K.; Dai, C.; Grover, D.; Zhang, S. Deduction of physicochemical properties from solubilities: 2,4-Dihydroxybenzophenone, biotin, and caprolactam as examples. *J. Chem. Eng. Data* **2015**, *60*, 1440–1446. [CrossRef]

25.   Hoover, K.R.; Acree, W.E., Jr.; Abraham, M.H. Chemical toxicity correlations for several fish species based on the Abraham solvation parameter model. *Chem. Res. Toxicol.* **2005**, *18*, 1497–1505. [CrossRef]

26.   Bowen, K.R.; Flanagan, K.B.; Acree, W.E., Jr.; Abraham, M.H.; Rafols, C. Correlation of the toxicity of organic compounds to tadpoles using the Abraham model. *Sci. Total Environ.* **2006**, *371*, 99–109. [CrossRef]

27.   Hoover, K.R.; Flanagan, K.B.; Acree, W.E., Jr.; Abraham, M.H. Chemical toxicity correlations for several protozoas, bacteria, and water fleas based on the Abraham solvation parameter model. *J. Environ. Eng. Sci.* **2007**, *6*, 165–174. [CrossRef]

28. Abraham, M.H.; Kumarsingh, R.; Cometto-Muniz, J.E.; Cain, W.S. An algorithm for nasal pungency thresholds in man. *Arch. Toxicol.* **1998**, *72*, 227–232. [CrossRef]

29. Poole, C.F.; Atapattu, S.N. Determination of physicochemical properties of ionic liquids by gas chromatography. *J. Chromatogr. A* **2021**, *1644*, 461964. [CrossRef]

30. Poole, C.F. Gas chromatography system constant database for 52 wall-coated, open-tubular columns covering the temperature range 60–140 °C. *J. Chromatogr. A* **2019**, *1604*, 460482. [CrossRef]

31. Poole, C.F. Evaluation of the solvation parameter model as a quantitative structure-retention relationship model for gas and liquid chromatography. *J. Chromatogr. A* **2020**, *1626*, 461308. [CrossRef]

32. Poole, C.F. Reversed-phase liquid chromatography system constant database over an extended mobile phase composition range for 25 siloxane-bonded silica-based columns. *J. Chromatogr. A* **2019**, *1600*, 112–126. [CrossRef] [PubMed]

33. Poole, C.F.; Lenca, N. Applications of solvation parameter model in reversed-phase liquid chromatography. *J. Chromatogr. A* **2017**, *1486*, 2–19. [CrossRef] [PubMed]

34. Abraham, M.H.; Kumarsingh, R.; Cometto-Muniz, J.E.; Cain, W.S. A quantitative structure-activity relationship (QSAR) for a Draize eye irritation database. *Toxicol. In Vitro* **1998**, *12*, 201–207. [CrossRef]

35. Abraham, M.H.; Hassanisadi, M.; Jalali-Heravi, M.; Ghafourian, T.; Cain, W.S.; Cometto-Muniz, J.E. Draize rabbit eye test compatibility with eye irritation thresholds in humans: A quantitative structure-activity relationship analysis. *Toxicol. Sci.* **2003**, *76*, 384–391. [CrossRef]

36. Zhao, Y.H.; Le, J.; Abraham, M.H.; Hersey, A.; Eddershaw, P.J.; Luscombe, C.N.; Boutina, D.; Beck, G.; Sherborne, B.; Cooper, I.; et al. Evaluation of human intestinal absorption data and subsequent derivation of a quantitative structure-activity relationship (QSAR) with the Abraham descriptors. *J. Pharm. Sci.* **2001**, *90*, 749–784. [CrossRef]

37. Zhao, Y.H.; Abraham, M.H.; Hersey, A.; Luscombe, C.N. Quantitative relationship between rat intestinal absorption and Abraham descriptors. *Eur. J. Med. Chem.* **2003**, *38*, 939–947. [CrossRef]

38. Abraham, M.H.; Martins, F. Human skin permeation and partition: General linear free-energy relationship analyses. *J. Pharm. Sci.* **2004**, *93*, 1508–1523. [CrossRef]

39. Zhang, K.; Abraham, M.H.; Liu, X. An equation for the prediction of human skin permeability of neutral molecules, ions and ionic species. *Int. J. Pharm.* **2017**, *521*, 259–266. [CrossRef]

40. Abraham, M.H.; Acree, W.E., Jr. The correlation and prediction of the temperature variation of infinite dilution activity coefficients of compounds in water. *Fluid Phase Equilib.* **2018**, *455*, 1–5. [CrossRef]

41. Abraham, M.H.; Acree, W.E., Jr.; Zissimos, A.M. The correlation and prediction of infinite dilution activity coefficients of compounds in water at 298.15 K. *Fluid Phase Equilib.* **2017**, *449*, 117–129. [CrossRef]

42. Mintz, C.; Clark, M.; Acree, W.E., Jr.; Abraham, M.H. Enthalpy of solvation correlations for gaseous solutes dissolved in water and in 1-octanol based on the Abraham model. *J. Chem. Inf. Model.* **2007**, *47*, 115–121. [CrossRef] [PubMed]

43. Stephens, T.W.; De La Rosa, N.E.; Saifullah, M.; Ye, S.; Chou, V.; Quay, A.N.; Acree, W.E., Jr.; Abraham, M.H. Enthalpy of solvation correlations for organic solutes and gases dissolved in 2-propanol, 2-butanol, 2-Methyl-1-propanol and ethanol. *Thermochim. Acta* **2011**, *523*, 214–220. [CrossRef]

44. Lu, J.Z.; Acree, W.E., Jr.; Abraham, M.H. Abraham model correlations for enthalpies of solvation of organic solutes dissolved in *N,N*-dimethylacetamide, 2-butanone and tetrahydrofuran (UPATED) at 298.15 K. *Phys. Chem. Liq.* **2020**, *58*, 675–692. [CrossRef]

45. Churchill, B.; Acree, W.E., Jr.; Abraham, M.H. Development of Abraham model expressions for predicting the standard molar enthalpies of vaporization of organic compounds at 298.15 K. *Thermochim. Acta* **2019**, *681*, 178372. [CrossRef]

46. Abraham, M.H.; Acree, W.E., Jr. Estimation of enthalpies of sublimation of organic, organometallic and inorganic compounds. *Fluid Phase Equilib.* **2020**, *515*, 112575. [CrossRef]

47. Abraham, M.H.; Acree, W.E., Jr. Estimation of vapor pressures of liquid and solid organic and organometallic compounds at 298.15 K. *Fluid Phase Equilib.* **2020**, *519*, 112595. [CrossRef]

48. Abraham, M.H.; Acree, W.E., Jr. Limiting diffusion coefficients for ions and nonelectrolytes in solvents water, methanol, ethanol, propan-1-ol, butan-1-ol, octan-1-ol, propanone and acetonitrile at 298 K, analyzed using Abraham descriptors. *J. Solut. Chem.* **2019**, *48*, 748–757. [CrossRef]

49. Hills, E.E.; Abraham, M.H.; Hersey, A.; Bevan, C.D. Diffusion coefficients in ethanol and in water at 298 K: Linear free energy relationships. *Fluid Phase Equilib.* **2011**, *303*, 45–55. [CrossRef]

50. Endo, S.; Goss, K.-U. Applications of polyparameter linear free energy relationships in environmental chemistry. *Environ. Sci. Technol.* **2014**, *48*, 12477–12491. [CrossRef]

51. Poole, C.F.; Ariyasena, T.C.; Lenca, N. Estimation of the environmental properties of compounds from chromatographic measurements and the solvation parameter model. *J. Chromatogr. A* **2013**, *1317*, 85–104. [CrossRef] [PubMed]

52. Jalan, A.; Ashcraft, R.W.; West, R.H.; Green, W.H. Predicting solvation energies for kinetic modeling. *Ann. Rep. Prog. Chem. Sect. C Phys. Chem.* **2010**, *106*, 211–258. [CrossRef]

53. He, J.; Abraham, M.H.; Acree, W.E., Jr.; Zhao, Y.H. A linear free energy analysis of PAMPA models for biological systems. *Int. J. Pharm.* **2015**, *496*, 717–722. [CrossRef] [PubMed]

54. Platts, J.A.; Butina, D.; Abraham, M.H.; Hersey, A. Estimation of molecular linear free energy relation descriptors using a group contribution approach. *J. Chem. Inf. Comp. Sci.* **1999**, *39*, 835–845. [CrossRef]

55. Platts, J.A.; Abraham, M.H.; Butina, D.; Hersey, A. Estimation of molecular linear free energy relationship descriptors by a group contribution approach. 2. Prediction of partition coefficients. *J. Chem. Inf. Comp. Sci.* **2000**, *40*, 71–80. [CrossRef] [PubMed]

56. Chung, Y.; Vermeire, F.H.; Wu, H.; Walker, P.J.; Abraham, M.H.; Green, W.H. Group contribution and machine learning approaches to predict Abraham solute parameters, solvation free energy, and solvation enthalpy. *J. Chem. Inf. Model.* **2022**, *62*, 433–446. [CrossRef]

57. Ulrich, N.; Ebert, A. Can deep learning algorithms enhance the prediction of solute descriptors for linear solvation energy relationship approaches? *Fluid Phase Equilib.* **2022**, *555*, 113349. [CrossRef]

58. Ulrich, N.; Endo, S.; Brown, T.N.; Watanabe, N.; Bronner, G.; Abraham, M.H.; Goss, K.-U. *UFZ-LSER Database v 3.2.1 [Internet]*; Helmholtz Centre for Environmental Research-UFZ: Leipzig, Germany, 2017; Available online: http://www.ufz.de/lserd (accessed on 17 May 2022).

59. Grubbs, L.M.; Saifullah, M.; De La Rosa, N.E.; Ye, S.; Achi, S.S.; Acree, W.E., Jr.; Abraham, M.H. Mathematical correlations for describing solute transfer into functionalized alkane solvents containing hydroxyl, ether, ester or ketone solvents. *Fluid Phase Equilib.* **2010**, *298*, 48–59. [CrossRef]

60. Bradley, J.-C.; Abraham, M.H.; Acree, W.E., Jr.; Lang, A.S.I.D. Predicting Abraham model solvent coefficients. *Chem. Cent. J.* **2015**, *9*, 12. [CrossRef]

61. Brown, T.N. Empirical regressions between system parameters and solute descriptors of polyparameter linear free energy relationships (PPLFERs) for predicting solvent-air partitioning. *Fluid Phase Equilib.* **2021**, *540*, 113035. [CrossRef]

62. Brown, T.N. QSPRs for predicting equilibrium partitioning in solvent–air systems from the chemical structures of solutes and solvents. *J. Solut. Chem.* **2022**, *in press*. [CrossRef]

63. Liu, G.; Eddula, S.; Jiang, C.; Huang, J.; Tirumala, P.; Xu, A.; Acree, W.E., Jr.; Abraham, M.H. Abraham solvation parameter model: Prediction of enthalpies of vaporization and sublimation of mono-methyl branched alkanes using measured gas chromatographic data. *Eur. Chem. Bull.* **2020**, *9*, 273–284. [CrossRef]

64. Tirumala, P.; Huang, J.; Eddula, S.; Jiang, C.; Xu, A.; Liu, G.; Acree, W.E., Jr.; Abraham, M.H. Calculation of Abraham model L-Descriptor and standard molar enthalpies of vaporization and sublimation for C_9–C_{26} mono-alkyl alkanes and polymethyl alkanes. *Eur. Chem. Bull.* **2020**, *9*, 317–328. [CrossRef]

65. Shanmugam, N.; Eddula, S.; Acree, W.E., Jr.; Abraham, M.H. Calculation of Abraham model L-descriptor and standard molar enthalpies of vaporization for linear C_7-C_{14} alkynes from gas chromatographic retention index data. *Eur. Chem. Bull.* **2021**, *10*, 46–57. [CrossRef]

66. Sinha, S.; Varadharajan, A.; Xu, A.; Wu, E.; Acree, W.E., Jr. Determination of Abraham model solute descriptors for hippuric acid from measured molar solubilities in several organic mono-solvents of varying polarity and hydrogen-bonding ability. *Phys. Chem. Liq.* **2022**, *60*, 563–571. [CrossRef]

67. Liu, X.; Aghamohammadi, A.; Afarinkia, K.; Abraham, R.J.; Acree, W.E., Jr.; Abraham, M.H. Descriptors for edaravone; studies on its structure, and prediction of properties. *J. Mol. Liq.* **2021**, *332*, 115821. [CrossRef]

68. Liu, X.; Abraham, M.H.; Acree, W.E., Jr. Descriptors for vitamin K3 (menadione); calculation of biological and physicochemical properties. *J. Mol. Liq.* **2021**, *330*, 115707. [CrossRef]

69. Xu, A.; Varadharajan, A.; Shanmugam, N.; Kim, K.; Huang, E.; Cai, S.K.; Acree, W.E., Jr. Abraham model description of the solubilising properties of the isopropyl acetate organic mono-solvent. *Phys. Chem. Liq.* **2022**, *60*, 312–324. [CrossRef]

70. Kim, K.; Shanmugam, N.; Xu, A.; Varadharajan, A.; Cai, S.K.; Huang, E.; Acree, W.E., Jr. Abraham model correlations for describing solute transfer into anisole based on measured activity coefficients and molar solubilities. *Phys. Chem. Liq.* **2022**, *60*, 452–462. [CrossRef]

71. Cai, S.K.; Huang, E.; Kim, K.; Shanmugam, N.; Varadharajan, A.; Xu, A.; Acree, W.E., Jr. Development of Abraham model correlations for solute transfer into cyclopentanol from both water and the gas phase based on measured solubility ratios. *Phys. Chem. Liq.* **2022**, *60*, 287–296. [CrossRef]

72. Katritzky, A.R.; Chen, K.; Maran, U.; Carlson, D.A. QSPR correlation and predictions of gc retention indexes for methyl-branched hydrocarbons produced by insects. *Anal. Chem.* **2000**, *72*, 101–109. [CrossRef] [PubMed]

73. Abraham, M.H.; McGowan, J.C. The use of characteristic volumes to measure cavity terms in reversed phase liquid chromatography. *Chromatographia* **1987**, *23*, 243–246. [CrossRef]

74. Chickos, J.S.; Hosseini, S.; Hesse, D.G. Determination of vaporization enthalpies of simple organic molecules by correlations of changes in gas chromatographic net retention times. *Thermochim. Acta* **1995**, *249*, 41–61. [CrossRef]

75. Chickos, J.S.; Wilson, J.A. Vaporization enthalpies at 298.15 K of the n-alkanes from C_{21} to C_{28} and C_{30}. *J. Chem. Eng. Data* **1997**, *42*, 190–197. [CrossRef]

76. Chickos, J.S.; Hanshaw, W. Vapor Pressures and vaporization enthalpies of the n-alkanes from C_{31} to C_{38} at T = 298.15 K by correlation gas chromatography. *J. Chem. Eng. Data* **2004**, *49*, 620–630. [CrossRef]

77. Nagrimanov, R.N.; Samatov, A.A.; Buzyurov, A.V.; Kurshev, A.G.; Ziganshin, M.A.; Zaitsau, D.H.; Solomonov, B.N. Thermochemical properties of mono- and di-cyano-aromatic compounds at 298.15 K. *Thermochim. Acta* **2018**, *668*, 152–158. [CrossRef]

78. Solomonov, B.N.; Varfolomeev, M.A.; Nagrimanov, R.N.; Novikov, V.B.; Buzyurov, A.V.; Fedorova, Y.V.; Mukhametzyanov, T.A. New method for determination of vaporization and sublimation enthalpy of aromatic compounds at 298.15K using solution calorimetry technique and group-additivity scheme. *Thermochim. Acta* **2015**, *622*, 88–96.

79. Solomonov, B.N.; Varfolomeev, M.A.; Nagrimanov, R.N.; Novikov, V.B.; Zaitsau, D.H.; Verevkin, S.P. Solution calorimetry as a complementary tool for the determination of enthalpies of vaporization and sublimation of low volatile compounds at 298.15 K. *Thermochim. Acta* **2014**, *589*, 164–173. [CrossRef]

80. Solomonov, B.N.; Nagrimanov, R.N.; Varfolomeev, M.A.; Buzyurov, A.V.; Mukhametzyanov, T.A. Enthalpies of fusion and enthalpies of solvation of aromatic hydrocarbons derivatives: Estimation of sublimation enthalpies at 298.15 K. *Thermochim. Acta* **2016**, *627–629*, 77–82. [CrossRef]

81. Solomonov, B.N.; Varfolomeev, M.A.; Nagrimanov, R.N.; Mukhametzyanov, T.A.; Novikov, V.B. Enthalpies of solution, enthalpies of fusion and enthalpies of solvation of polyaromatic hydrocarbons: Instruments for determination of sublimation enthalpy at 298.15 K. *Thermochim. Acta* **2015**, *622*, 107–112. [CrossRef]

82. Lu, J.Z.; Acree, W.E., Jr.; Abraham, M.L. Updated Abraham model correlations for enthalpies of solvation of organic solutes dissolved in benzene and acetonitrile. *Phys. Chem. Liq.* **2019**, *57*, 84–99. [CrossRef]